COMPARATION OF FUSION METHODS ON GF-5 HYPERSPECTRAL DATA

Xiaoyang Zhao (1)(2), Lifu Zhang (1), Xuejian Sun (1), Yi Cen (1)

[1] Aerospace Information Research Institute, Chinese Academy of Sciences, 20 Datun road, Chaoyang District, Beijing 100101, China;
[2] University of Chinese Academy of Sciences, 19 Yuquan Road, Shijingshan District, Beijing, 100049, China
Email: zhaoxy@radi.ac.cn; zhanglf@radi.ac.cn; sunxj@radi.ac.cn; cenyi@radi.ac.cn

ABSTRACT: Data fusion is an effective way to solve the limitation of hyperspectral satellites on temporal and spatial resolution. It is of great significance to discuss the fusion effects of different methods on GF-5 hyperspectral data for information mining and promotion application of GF-5 hyperspectral data.In this study, based on the principle that the algorithm is easy to use and suitable for generalization, six fusion methods, GS (Gram-Schmidt), GSA (GS Adaptive), CNMF (Coupled Non-negative Matrix Factorization), CRISP-B, CRISP-W (Color Resolution Improvement Software Package with Butterworth or Wavelet transform), GLP (Generalized Laplacian Pyramid) are respectively used to perform fusion experiments on GF-5 hyperspectral data and multispectral data from BJ-2, GF-2, and GF-1/1C/1D domestic satellites. Visual interpretation, five indicators (Correlation Coefficient, Universal Image Quality Index, Spectral Angle Mapper, Erreur Relative Globale Adimensionnelle de Synthèse and Peak Signal to Noise Ratio), classification application and time costs are used to comprehensively evaluate the fusion results.The results show that the fusion image series are the same and the smaller the spatial resolution difference is, the better the fusion result is. CRISP-B, CRISP-W, GLP can achieve a good balance in improving spatial resolution and spectral fidelity. In terms of spatial reconstruction, GLP is slightly better and more stable, while CRISP-B and CRISP-W are more stable and effective in maintaining spectral information. The data source will have a certain impact on the fusion method. In the tasks that require high spectral fidelity, such as spectral feature information extraction and analysis, GLP is more suitable for the fusion of homologous data (such as GF-5 and GF-1/1C/1D/2). When the multi-source images (GF-5 and BJ-2) are merged, CRISP-W is preferred. CNMF has a certain degree of color distortion and takes a long time to run. GSA and GS have the worst fusion effect. Both the spectral retention and the spatial resolution improvement ability of GSA are more stable than GS's. Based on small sample, the classification effect of CRISP-B fusion result is stable and high-accuracy. The GSA fusion results are rich in spatial details. Although the spectral distortion is relatively serious, it also increases the spectral distinction of the ground objects, which is still suitable for accurately drawing buildings, roads.This study provides method decision support for the fusion of GF-5 hyperspectral data and other domestic satellite multispectral data, which is helpful for the application and promotion of GF-5 hyperspectral data.

KEY WORDS: domestic satellite, data fusion, fusion method evaluation

1. Introduction

The Gaofen-5 (GF-5) satellite was successfully launched on May 9th, 2018. It is the first satellite in China to achieve high spectral resolution observation in the Major Project of High Resolution Earth Observation System, and it is the world's first full-spectrum hyperspectral satellite to make comprehensive observations of the atmosphere and land (Sun et al., 2018). The spatial resolution of GF-5 hyperspectral data is 30 meters (Liu et al., 2018). Compared with multispectral satellites such as Gaofen-1 (GF-1) and Gaofen-2 (GF-2), its spatial resolution is still insufficient in many applications (Li et al., 2018). Using spatial-spectral fusion methods to fuse

hyperspectral data with panchromatic or multispectral images (MSI) is an effective technical method to improve the spatial resolution of hyperspectral images (HSI) (Tong et al., 2014). Therefore, it is of great significance to discuss the fusion effects of different methods on GF-5 hyperspectral data for information mining and promotion application of GF-5 hyperspectral data.

Yokoya et al. studied the fusion performance of the latest 10 fusion methods on hyperspectral and multispectral data (Yokoya et al., 2017). This study provides a good direction for the fusion of hyperspectral and multispectral data. However, this study only used simulated hyperspectral data, so the conclusion was limited in practical applications, such as different hardware design of GF-5 imager, different spatial resolution, and actual acquisition geometry. Ren Kai et al. fused GF-5 hyperspectral data with GF-1, GF-2, Sential-2A multispectral data, and comprehensively evaluated the performance of nine fusion methods (Ren et al., 2020). However, it involves fewer domestic multi-spectral satellite data sources, such as not involving Beijing-2 (BJ-2), GF-1C, GF-1D, etc.

In this study, based on the principle that the algorithm is easy to use and suitable for generalization, six fusion methods, Gram-Schmidt (GS), GS Adaptive (GSA), Coupled Non-negative Matrix Factorization (CNMF), Color Resolution Improvement Software Package with Butterworth (CRISP-B) or Wavelet transform (CRISP-W), Generalized Laplacian Pyramid (GLP) are respectively used to perform fusion experiments on GF-5 hyperspectral data and multispectral data from BJ-2, GF-2, and GF-1/1C/1D domestic satellites. Visual interpretation, five indicators, including Correlation Coefficient (CC), Universal Image Quality Index (UIQI), Spectral Angle Mapper (SAM), Erreur Relative Globale Adimensionnelle de Synthèse (ERGAS) and Peak Signal to Noise Ratio (PSNR), and classification application as well as time costs are used to comprehensively evaluate the fusion results.

This study provides method decision support for the fusion of GF-5 hyperspectral data and other domestic satellite multispectral data, which is helpful for the application and promotion of GF-5 hyperspectral data.

2. Experiment

The multispectral data of GF-1/1C/1D, GF-2, and BJ-2 from Poyang Lake, the Yellow River estuary, and Dongting Lake area, as well as GF-5 hyperspectral data of the same area at similar time were fused separately. The data are shown in Table 1.

Table 1 Experiment data

ID	Area	Center Longitude	Center Latitude	Multispectral Sensor (Spatial resolution)	Date	Hyperspectral Sensor (Spatial resolution)	Date
A	Poyang Lake	116.39E	28.77N	BJ-2 (4m)	20181002	GF-5 (30m)	20181005
B	Dongting Lake	112.63E	28.67N	GF-2 (4m)	20181005		20181005
C	Poyang Lake	116.31E	28.75N	GF-1 (8m)	20181006		20181007
D	Poyang Lake	116.44E	28.72N	GF-1C (8m)	20181008		20181007
E	The Yellow River estuary	118.94E	37.60N	GF-1D (8m)	20181103		20181101
F	Dongting Lake	112.63E	28.67N	GF-1D (8m)	20181006		20181005

The experiment data includes typical features such as bare soil, buildings, roads, water bodies, farmland, breeding areas, paddy field and farmland. The image data are all Level-1 products, and the pixels are radiance values. ENVI is used to preprocess each group data (A-F) separately. Firstly, RPC orthorectification module is used to orthorectify the multispectral and hyperspectral data, the GF-5 hyperspectral data is resampled to 4m in the A-B group, and 8m in the C-F group. Then multispectral data is regarded as the reference image and the hyperspectral data as the image to be registered. The homonymy points are selected, and each group of images are registered. Finally, the same area of 400 × 400 pixels is selected for fusion experiments.

Among them, the filter function of GS is the spectral response function; the preset pure pixels number of CNMF is automatically determined by the virtual dimension method; the CRISP cut-off frequency is 20, and the number of wavelet filter layers of the CRISP-W is 3; GLP uses the

least square method to calculate the regression coefficient matrix.

3. Results

3.1 Visual analysis

In order to facilitate visual interpretation and qualitative evaluation, the fusion results are displayed in true color images with the same band combination (GF-1/1C/1D, R: Band3 680nm, G: Band2 576nm, B: Band1 502nm; GF-2, R: Band3 660nm, G: Band2 555nm, B: Band1 485nm; BJ-2, R: Band3 635nm, G: Band2 550nm, B: Band1 475nm; GF-5 and fusion image, R: Band59 638.4nm, G: Band38 548.47nm, B: Band17 458.59nm), the stretching method also remains the same (Fig.1).

In general, GS cannot effectively improve the spatial resolution, and the fusion result is the fuzziest, especially in A, B, C, D, and F, where the ground features are broken and complex. CNMF has obvious color distortions, which are shown in the six groups of experiments. Both GSA and GLP can effectively improve the spatial resolution. The texture of the ground features is clearer, but the performance of the color fidelity is slightly different. In B, C, E, and F, the color of the GSA fusion result is similar to the multispectral image. The color of the GLP fusion result is closer to the hyperspectral data, which shows to a certain extent that the spectral fidelity of GLP is better than GSA. The fusion results of CRISP-B and CRISP-W methods are relatively close, and the hue is natural. All 6 groups of experiments show good spectral retention ability, but the spatial resolution improvement ability is not as good as GLP.

In summary, when the types of ground boundary rules are relatively simple, the six methods are not much different. When the type of ground fragmentation is complex, the spectral retention ability of GLP, CRISP-B, CRISP-W is better, and the spatial resolution improvement ability of GLP, GSA is better. GS cannot effectively improve the spatial resolution, and there is color distortion in the CNMF fusion results.

3.2 Index evaluation

Table 2 shows the relevant index values of the results generated based on different experimental data and different fusion methods. In longitudinal comparison, it can be seen that groups C, D, E, and F are closer to groups A, B. CC, and UIQI are closer to 1; PSNR is larger, and SAM is smaller. That is, the fused image is more related to the reference image, the brightness and contrast are more similar, and the spatial reconstruction quality and spectrum retention ability are better. This is because the two groups of experiments in A and B are all fused with a multispectral image with a spatial resolution of 4m and a hyperspectral image with a spatial resolution of 30m, while the four groups of experiments with C, D, E, and F are all 8m multispectral images and 30m hyperspectral image fusion. The ERGAS performance is relatively abnormal. This is because the data in Group E has a large range of water, and the average pixel value in the image band is low, which makes the ERGAS value too large. Therefore, when compared between experimental groups, the ERGAS index should not be relied on too much. It is not difficult to find that GF-2 is better than BJ-2 data in the fusion experiment with a spatial resolution of 4m in multispectral data; and in the 8m experiment, GF-1D data performs better. In summary, the smaller the difference in the spatial resolution of a group of fused images, the better the fusion effect. When fusing GF-5 hyperspectral data with 4m multispectral data, GF-2 can be preferentially selected, and when fusing with 8m multispectral data, GF-1D can be preferentially selected. A horizontal comparison, that is, a comparison between different fusion methods. In terms of spatial reconstruction, GLP is the best. The performance of CRISP-B and CRISP-W are relatively good. Especially when fusing GF-5 and BJ-2, in these three fusion results, CC have reached 0.84; UIQI have reached 0.81 and PSNR are above 24.5. This shows that the image source has little influence on the spatial reconstruction ability of CRISP-B, CRISP-W, and GLP. In terms of spectral retention, CNMF, GLP, CRISP-B and CRISP-W all showed good results. CRISP-W is slightly better than CRISP-B; the average of both SAM are higher, and the standard deviation are very low, thus the performances are stable. GLP and CNMF have the highest SAM average, but the standard deviation is large, which is mainly affected by the A group multi-source fusion

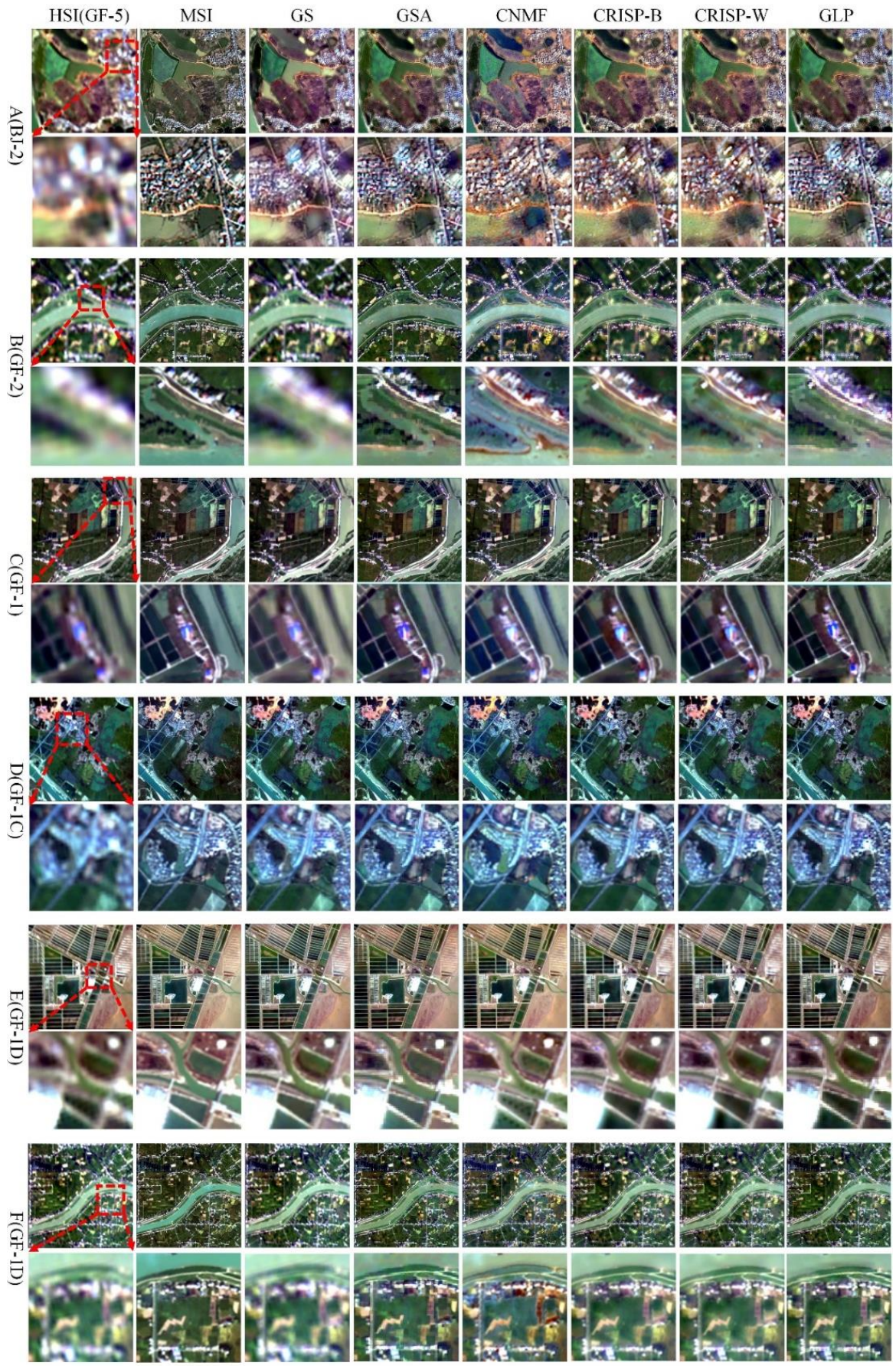

Note: On the left, A-F number the experienments and the sensors noted in brackets are the multispectral data sources.

Fig.1 Fusion results of different methods and data

Table 2 Evalution Indexes of fusion results

CC	GS	GSA	CNMF	CRISP-B	CRISP-W	GLP	Mean
A	0.59	0.74	0.75	0.84	0.84	0.87	0.77
B	0.92	0.83	0.86	0.88	0.89	0.94	0.89
F	0.94	0.89	0.87	0.93	0.93	0.92	0.91
E	0.92	0.92	0.92	0.96	0.96	0.95	0.94
D	0.97	0.94	0.91	0.96	0.96	0.96	0.95
C	0.97	0.95	0.94	0.95	0.95	0.96	0.95
Mean	0.89	0.88	0.87	0.92	0.92	0.93	
Std	0.13	0.07	0.06	0.04	0.04	0.03	
UIQI	GS	GSA	CNMF	CRISP-B	CRISP-W	GLP	Mean
A	0.58	0.70	0.74	0.81	0.82	0.85	0.75
B	0.91	0.81	0.85	0.87	0.88	0.93	0.88
F	0.94	0.88	0.86	0.92	0.93	0.91	0.91
E	0.92	0.91	0.92	0.96	0.96	0.95	0.94
D	0.97	0.94	0.91	0.95	0.96	0.96	0.95
C	0.97	0.95	0.93	0.94	0.95	0.96	0.95
Mean	0.88	0.87	0.87	0.91	0.91	0.93	
Std	0.14	0.09	0.06	0.05	0.05	0.04	
PSNR	GS	GSA	CRISP-B	CRISP-W	CNMF	GLP	Mean
A	21.57	21.18	24.54	25.01	23.39	25.17	23.48
B	32.21	23.92	25.84	26.55	26.28	29.00	27.30
E	27.61	26.79	29.74	30.06	27.58	29.03	28.47
F	38.78	27.36	29.29	29.74	28.23	28.76	30.36
C	34.19	29.72	29.44	30.33	29.66	31.37	30.79
D	32.91	30.23	31.16	31.85	29.54	31.55	31.21
Mean	31.21	26.53	28.34	28.93	27.45	29.15	
Std	5.42	3.17	2.34	2.36	2.15	2.11	
SAM	GSA	GS	CNMF	GLP	CRISP-B	CRISP-W	Mean
A	4.49	4.31	2.85	2.77	2.33	2.17	3.15
B	3.20	3.74	1.79	1.78	2.36	2.11	2.50
F	2.48	2.36	1.49	2.06	2.13	1.95	2.08
E	2.56	2.20	1.98	1.85	1.83	1.75	2.03
C	2.20	1.67	1.94	1.72	2.13	1.88	1.92
D	1.94	1.06	1.81	1.68	1.83	1.63	1.66
Mean	2.81	2.56	1.98	1.98	2.10	1.91	
Std	0.84	1.13	0.42	0.38	0.21	0.19	
ERGAS	GS	GSA	CNMF	GLP	CRISP-B	CRISP-W	Mean
E	4.14	4.10	3.49	3.50	3.26	3.10	3.60
F	2.31	2.29	1.80	1.91	1.80	1.68	1.97
C	2.07	2.12	2.00	1.71	2.04	1.84	1.96
A	2.90	2.29	1.61	1.51	1.40	1.31	1.84
D	1.63	1.88	1.85	1.66	1.68	1.54	1.71
B	1.67	1.55	1.05	0.87	1.15	1.05	1.22
Mean	2.45	2.37	1.97	1.86	1.89	1.75	
Std	0.87	0.81	0.75	0.80	0.68	0.65	

Note: Based on each index, the average value of the index indicating the fusion result from white to red is low to high, and the standard deviation of the index indicating the fusion result from white to blue is small to large. From top to bottom, white to green indicates that the index values of the experimental groups become better. In each set of experiments for each index, the better the index value, the higher the gray level. CC, UIQI, and PSNR are all band averages, and SAM is the pixel average.

experiment. Therefore, in order to better maintain the spectral information, GLP can be preferentially selected when fusing between homologous data, and CRISP-W is preferentially used when fusing between multi-source data. The spatial reconstruction ability and spectral retention ability of GS and GSA are both poor, especially in Experiment A. Although the GS method performs better in the four groups (BCDF) experiments, such as the average of the CC and UIQI of the four groups are about 0.95, the average value of PSNR reaches the highest, but this is because the GS method fails to effectively remove the noise value of the hyperspectral data. The content of this part will be explained in detail in the discussion part. In addition, GSA is more stable than GS in both spectral retention and spatial resolution improvement. ERGAS is a comprehensive index, which has certain advantages when using images with certain registration errors as reference images. In summary, combined with the comprehensive index ERGAS, it can be concluded that the CRISP-W method is the best and the most stable; CRISP-B and GLP are

slightly less effective; CNMF is in the middle, and GS and GSA are the worst.

Table 3 Runtimes comparison of different fusion methods

Test (s)	GS	GSA	CRISP-W	GLP	CRISP-B	CNMF
A	ENVI Interaction	5.4	8.6	13.5	16.4	417.3
B		5.0	8.6	13.4	16.1	422.9
C		5.0	8.7	13.3	16.4	426.0
D		5.0	8.6	13.4	16.1	474.2
E		5.0	8.8	13.6	16.7	466.0
F		5.0	8.7	14.7	16.6	442.4
Mean		5.1	8.7	13.7	16.4	441.5

As can be seen from Table 3, the running time of GSA, CRISP-W, GLP, CRISP-B, and CNMF increases in sequence, and the running time of CNMF is too long to be desirable. The operating costs of the other five methods are within the acceptable range.

3.3 Classification application

The landscape type of image has a great influence on the evaluation results. The diversity of landscape size and natural features leads to highly variable spatial and spectral information. Table 4 shows the label categories in the A, B, C, D, and F study areas and the number of specific samples used for training and testing. The number of samples in each category is equal, which avoids the different proportion of ground features to affect the evaluation results. There are few types of features in the E study area. In order to ensure the effectiveness of the method comparison, E is not classified. In addition, the classification results of fusion images can be identified more effectively when the ground truth is fine or the main ground features are boundaries.

Table 5 shows the original multispectral and hyperspectral images in different study areas, the overall classification accuracy of each fusion result, and Kappa coefficient. The classification result of GS is the worst, because GS has the worst spatial resolution improvement ability, which affects classification, especially fine classification. The effects of CNMF, GLP and CRISP-W are centered, among which, groups C, D, and F are better than groups A and B. This may be due to the small difference in spatial resolution of the images to be fused in groups C, D, and F, and the fusion results are relatively good, so the classification results are relatively better. In the two groups A and B, GSA showed strong superiority. Although the spectral retention of the GSA fusion result is poor, the component substitution increases the spectral divergence of the ground features. It is also found in visual analysis, the spatial information of GSA is closer to the multispectral image, and the spatial resolution has been effectively improved, thereby improving the precision of fine classification. CRISP-B has shown good results in the classification of all fusion results. When the number of samples is small, the overall accuracy of the original GF-5 classification results is improved by about 4 percentage points. Figure 2 shows the ground truth, classification results of hyperspectral and multispectral images, and CRISP-W, GSA, CRISP-B fusion image classification results with relatively good results. It can be seen that in the two groups of A and B, the road division by GSA is very clear, and the roads separated by CRISP-B and CRISP-W are thicker, and some are in the form of sheets. The green land and bare soil separated by CRISP-B etc. are basically lumpy. In the two groups C and D, the classification results of GSA are relatively broken. In group F, there is high classification accuracy of buildings and roads by GSA fusion, making the overall classification effect good.

In summary, the classification accuracy of different fusion methods is not significantly different for water bodies with a large degree of discrimination. For buildings and roads with broken ground features and borders that are difficult to identify, the classification effect of GSA fusion results is the best, but GSA will also partially break up flaky ground objects such as bare soil and farmland. The result of CRISP-B fusion results is stable, and the overall classification accuracy is high.

Table 4 Evalution Indexes of fusion results

Test (pixels)	Bearing land		Building		Roads		Water body		farmland		Breeding area		Paddy field	
	Tr	Te	Tr	Te	Tr	Te	Tr	Te	Tr	Te	Tr	Te	Tr	Te
A	30	970	30	970	30	970	30	970	30	970	/	/	/	/
B	30	970	30	970	30	970	30	970	30	970	/	/	/	/
C	30	970	30	970	30	970	30	970	30	970	30	970	30	970
D	30	970	30	970	30	970	30	970	30	970	30	970	30	970
F	30	970	30	970	30	970	30	970	30	970	30	970	/	/

Note: Tr means train; Te means test.

Table 5 Overall Occuracy (OA) and Kappa coefficient

Criterion	Test	HSI	MSI	GS	CNMF	GLP	CRISP-W	GSA	CRISP-B
OA (%)	A	81.32	87.96	87.84	87.46	85.57	86.04	88.72*	88.39*
	B	81.09	82.08	78.14	79.98	81.24	81.05	88.29***	83.59*
	C	88.26	86.41	86.52	87.78	88.06	88.92*	84.36	90.06***
	D	88.47	90.66	90.03	92.64*	92.53*	92.75*	90.24	93.43**
	F	88.76	90.55	88.47	91.56	90.86	92.11*	94.06***	93.25**
Kappa	A	0.767	0.850	0.848	0.843	0.820	0.826	0.859*	0.855*
	B	0.764	0.776	0.727	0.750	0.766	0.763	0.854***	0.795*
	C	0.863	0.841	0.843	0.857	0.861	0.871*	0.818	0.884**
	D	0.866	0.891	0.884	0.914*	0.913*	0.916*	0.886	0.923**
	F	0.865	0.887	0.862	0.899	0.890	0.905*	0.929***	0.919**

Note: the more *, the better the classification effect.

4. Discussion

(1) The CRISP model uses Wavelet and Butterworth filters to perform the frequency domain filtering process. The advantage of wavelet filter is that the processing speed is relatively fast, but when the image registration accuracy is low, there will be obvious "patches" in the fused image. Butterworth filter is relatively less affected by the accuracy of registration, showing a strong stability. In this case, the experimental data registration accuracy is higher, CRISP-W effect is better than CRISP-B, which shows the necessity of strict registration before fusion. However, whether it is a Wavelet filter or a Butterworth filter, different fusion images need different filter parameters to achieve the best fusion effect, thereby making it difficult to choose the basis function, filter cut-off frequency, and number of decomposition layers. The selected parameters are not ideal, and will cause further information loss in the fusion image space and spectrum. The main reason for these problems is that the image reconstruction process in the CRISP model is entirely based on mathematical statistics theory, and statistical optimization is performed mathematically. The lack of a clear physical meaning makes it easy to cause unstable results. In addition, in the CRISP model, the simulation process of the high spatial resolution hyperspectral image and the subsequent filtering process are completely independent two parts. If the hyperspectral data with high spatial resolution can be directly reconstructed without the need for filter fusion process, it will be an important improvement to the CRISP algorithm.

(2) In the process of band transformation, the GSA fusion algorithm will cause loss of spectral information and produce spectral distortion. A good fusion algorithm can not only increase the spatial texture information of the image, but also keep the original information of the spectrum. That is, no or little information distortion occurs. However, there is no absolute correlation between the fusion quality of various fusion methods, that is, spectrum, spatial fidelity and remote sensing applications. The results of this experiment show that the GSA spectrum is seriously distorted, but at the same time increases the spectral separation of ground features, and is particularly suitable for the classification of roads and buildings. In the next step, the fusion algorithm can be further analyzed for different application purposes such as vegetation monitoring, land productivity inversion, environmental assessment, mineral exploration, and target detection.

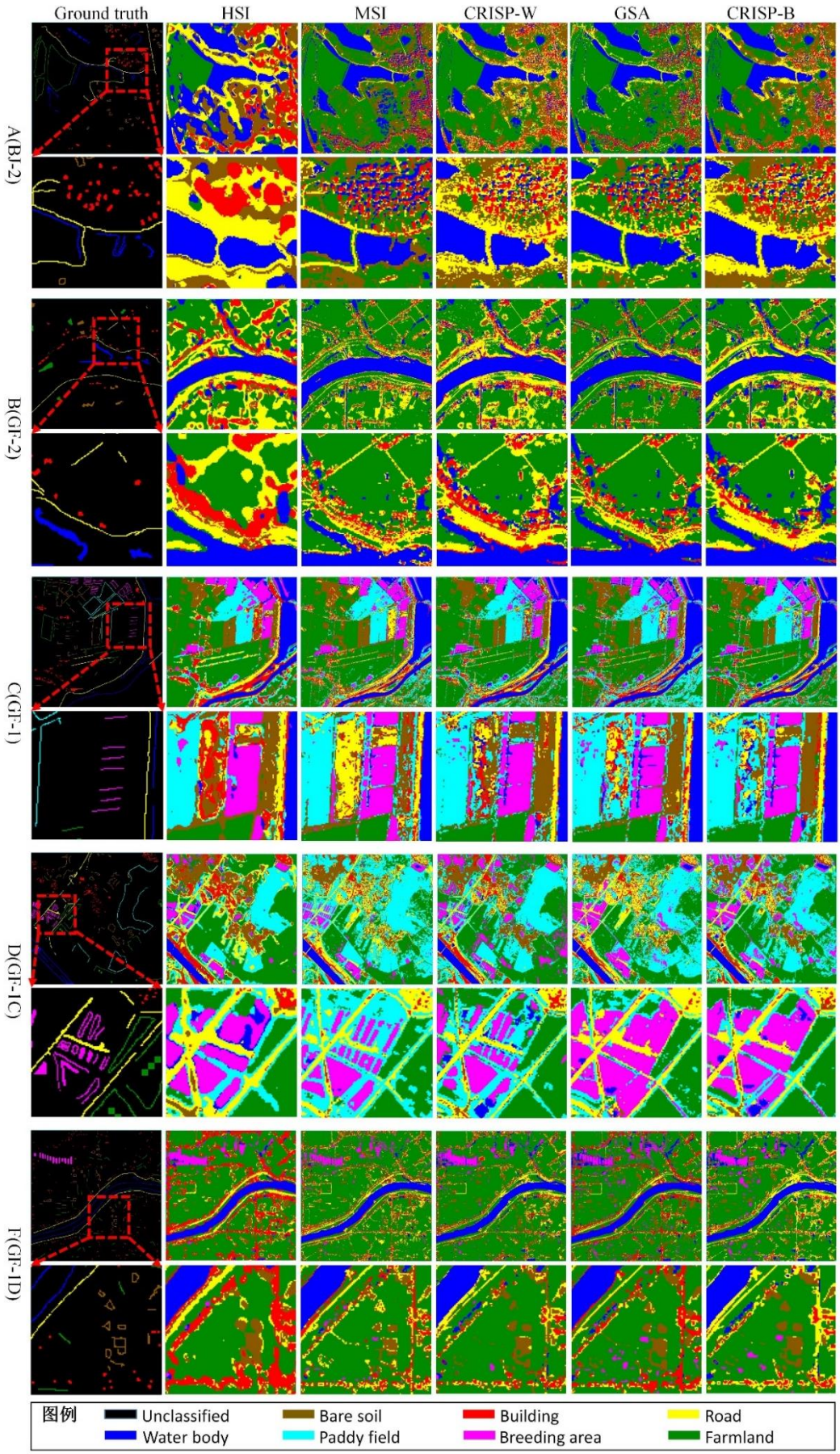

Note: A-D and F number the experienments. The sensors noted in brackets are the multispectral data sources.

Fig.2 Classification result

(3) Observing the original hyperspectral image, it is found that except for group E, bands in the front part of other five groups images have different levels of noise and stripes, and the quality is poor. It can also be seen from Figure 3 (methods are discussed here of which the spectrum holding effect is better and most stable), and the CC trend of Group E is the steadiest. In the other five sets of experiments, the CC values of the front bands of CRISP-B and CRISP-W all have increasing trends. This is because based on the fusion of CRISP-B and CRISP-W, image noise and stripes are greatly improved, which is quite different from the original image (Figure 4). Therefore, the CC value is lower, which is in line with the actual situation. However, the GS method has remained flat; that is, it is very similar to the original noisy image, and does not have the effect of CRISP-B and CRISP-W to remove noise. In the A, B, C, and F experiments, the CC of the GS method has a steep downward trend after about the 80th band (center wavelength 728.06nm), while other methods have an upward trend and maintain a relatively stable. The state, to a certain extent, shows that CRISP-B and CRISP-W have a retention advantage over the GS in the infrared band.

(4) The CNMF model meets the non-negative constraints of the linear mixed model. Because the objective function has obvious non-convexity, the model has a large number of convergence points; it may converge to a local minimum, resulting in a non-unique decomposition matrix. This may be the reason for the poor fusion effect of CNMF fusion in this case. In addition, CNMF needs to preset the number of unmixed end-members. Different preset methods will lead to different results. The influence of the preset end-member methods on the fusion result can be further explored.

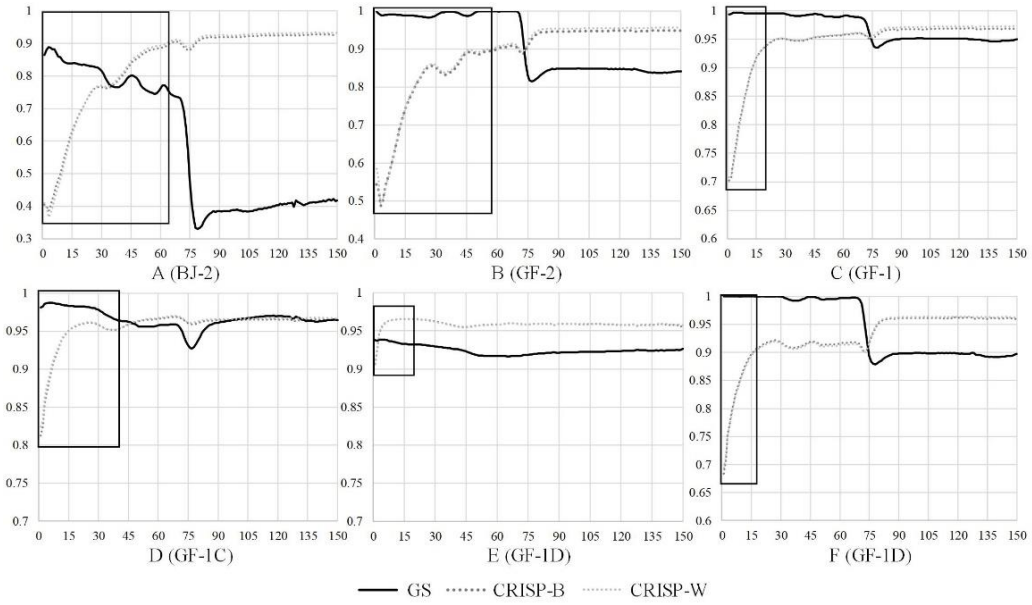

Fig.3 CC trend of different bands

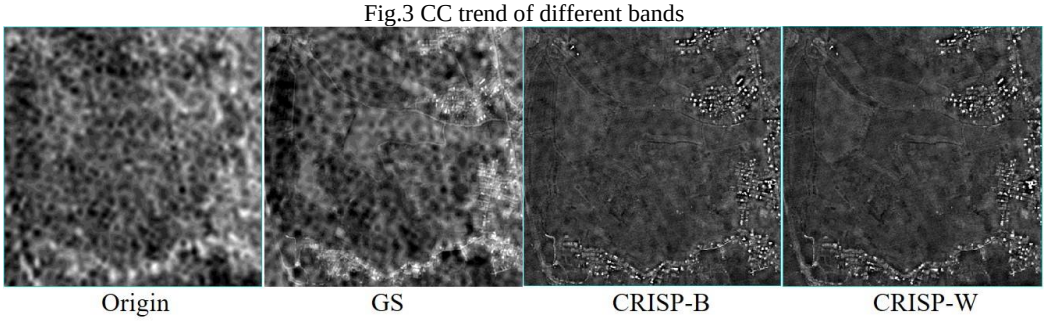

Fig.4 The first band image of origin and fusion result of test A

5. Conclusion

This study selects six simple and easy-to-promote hyperspectral fusion methods to fuse multiple domestic satellite multispectral data with GF-5 hyperspectral data. Through visual analysis, five classic evaluation indicators, classification application accuracy, and running time cost, the advantages and disadvantages of the fusion method are comprehensively analyzed. The results show that the fusion image series are the same and the smaller the spatial resolution difference is, the better the fusion result is. CRISP-B, CRISP-W, GLP can achieve a good balance in improving spatial resolution and spectral fidelity. In terms of spatial reconstruction, GLP is slightly better and more stable, while CRISP-B and CRISP-W are more stable and effective in maintaining spectral information. The data source will have a certain impact on the fusion method. In the tasks that require high spectral fidelity, such as spectral feature information extraction and analysis, GLP is more suitable for the fusion of homologous data (such as GF-5 and GF-1/1C/1D/2). When the multi-source images (GF-5 and BJ-2) are merged, CRISP-W is preferred. CNMF has a certain degree of color distortion and takes a long time to run. GSA and GS have the worst fusion effect. Both the spectral retention and the spatial resolution improvement ability of GSA are more stable than GS's. Based on small sample, the classification effect of CRISP-B fusion result is stable and high-accuracy. The GSA fusion results are rich in spatial details. Although the spectral distortion is relatively serious, it also increases the spectral distinction of the ground objects, which is still suitable for accurately drawing buildings, roads. This study provides a basis for method selection for the application research of GF-5 hyperspectral data in fusion.

References

Chen Z X, Ren J Q, Tang J H, Shi Y, Leng P, Liu J, Wang L M, Wu W B and Yao Y M. 2016. Progress and perspectives on agricultural remote sensing research and applications in China. Journal of Remote Sensing, 20(5): 748-767 [doi: 10.11834/jrs.20166214]

Huang, B, Zhang H K., Song H H, Wang J and Song C Q. 2013. Unified fusion of remote-sensing imagery: Generating simultaneously high-resolution synthetic spatialtemporalspectral earth observations. Remote Sensing Letters, 4(4-6): 561-569 [doi: 10.1080/2150704X.2013.769283]

Li X T, Lu J X, Song X N, Sun Y Y, Li L, Lei T J and Qu W. 2018. Application of the GF Satellite Data in Flood Disaster Monitoring. 7293-7296 [doi:10.1109/IGARSS.2018.8519548]

Liu Y N. 2018. Visible-shortwave Infrared Hyperspectral Imager of GF-5 Satellite. Spacecraft Recovery & Remote Sensing, 39(3): 25-28 [doi:10.3969/j.issn.1009-8518.2018.03.003]

Pohl C and Van G J L. 1998. Review article Multisensor image fusion in remote sensing: concepts, methods and applications. International Journal of Remote Sensing, 19(5): 823–854 [DOI: 10.1080/014311698215748]

Ren K, Sun W, Meng X, Yang G and Du Q. 2020. Fusing China GF-5 Hyperspectral Data with GF-1, GF-2 and Sentinel-2A Multispectral Data: Which Methods Should Be Used? Remote Sensing, 12(5): 882-907 [doi:10.3390/rs12050882]

Sun Y Z, Jiang G W, Li Y D, Yang Y, Dai H S, He J, Ye Q H, Cao Q, Dong C Z, Zhao S H and Wang W H. 2018. GF-5 Satellite: Overview and Application Prospects. Spacecraft Recovery & Remote Sensing, 39(3): 1-13 [doi:10.3969/j.issn.1009-8518.2018.03.001]

Tang J H, Wu W B, Yang P, Zhou Q B and Chen Z X. 2010. Advances research on remote sensing monitoring of crop spatial patterns. Scientia Agricultura Sinica, 43(14): 2879-2888 [doi:10.3864/j.issn.0578-1752.2010.14.006]

Tong Q, Xue Y and Zhang L. 2014. Progress in Hyperspectral Remote Sensing Science and Technology in China Over the Past Three Decades. IEEE Journal of Selected Topics in Applied Earth Observations and Remote Sensing, 7(1): 70-91 [doi:10.1109/jstars.2013.2267204]

Tong Q X, Zhang B and Zhang L F. 2016. Current progress of hyperspectral remote sensing in China. International Journal of Remote Sensing, 20(5):689-707 [doi: 10.11834/jrs.20166264]

Wang J Y, Wang Y M, Li C L. 2010. Noise model of hyperspectral imaging system and influence on radiation sensitivity. International Journal of Remote Sensing,14(4):614-628 [doi: 10.11834/jrs.20100401]

Wang J Y, Shu R and Liu Y N. 2011. Introduction to Imaging Spectroscopy. Science Press.

Yokoya N, Grohnfeldt C and Chanussot J. 2017. Hyperspectral and Multispectral Data Fusion: A comparative review of the recent literature. IEEE Geoscience and Remote Sensing Magazine, 5(2): 29-56 [doi: 10.1109/MGRS.2016.2637824]

Zhang L P and Shen H F. 2016. Progress and future of remote sensing data fusion. Journal of Remote Sensing, 20(5): 1050–1061 [DOI: 10.11834/jrs.20166243]

Zhu X L, Chen J, Gao F, Chen X H and Masek J G. 2010. An enhanced spatial and temporal adaptive reflectance fusion model for complex heterogeneous regions. Remote Sensing of Environment, 114(11): 2610-2623 [doi: 10.1016/j.rse.2010.05.032]